REVIEW

National Science Review
4: 121–135, 2017
doi: 10.1093/nsr/nww029
Advance access publication 28 April 2016

PHYSICS

Structure and superconductivity of hydrides at high pressures

Defang Duan, Yunxian Liu, Yanbin Ma, Ziji Shao, Bingbing Liu and Tian Cui*

State Key Laboratory of Superhard Materials, College of physics, Jilin University, Changchun 130012, China

***Corresponding author.** E-mail: cuitian@jlu.edu.cn

Received 21 January 2016; **Revised** 24 March 2016; **Accepted** 27 April 2016

ABSTRACT

Hydrogen atoms can provide high phonon frequencies and strong electron–phonon coupling in hydrogen-rich materials, which are believed to be potential high-temperature superconductors at lower pressure than metallic hydrogen. Especially, recently both of theoretical and experimental reports on sulfur hydrides under pressure exhibiting superconductivity at temperatures as high as 200 K have further stimulated an intense search for room-temperature superconductors in hydrides. This review focuses on crystal structures, stabilities, pressure-induced transformations, metallization, and superconductivity of hydrogen-rich materials at high pressures.

Keywords: superconductivity, metallization, crystal structure, high pressure, hydride

INTRODUCTION

Since superconductivity of 4.2 K in mercury was first discovered by Onnes in 1911 [1], searching for high critical temperature superconductors has been one of the major activities in condensed matter physics. There is a great progress in the study of unconventional superconductors such as copper oxides and iron-based compounds which often show high superconducting transition temperature (T_c). Although their superconducting mechanisms are still a controversy, the highest T_c of copper oxides and iron-based superconductors reach 133 K [2] and 56 K [3] at ambient pressure, respectively. But the situation is not optimistic for the conventional superconductors. Magnesium diboride—the best known conventional superconductor with T_c of 39 K [4] observed in 2001 is far lower than that of copper oxide superconductor.

Pressure is one of the thermodynamic parameters that controls the structures and properties of condensed matter. High pressure can effectively reduce the distance between atoms, shorten the bonds, and change electronic structure, leading to new phases with unusual structures and properties that hardly occur at atmospheric pressure. For example, high pressure can make the insulator transform to a metal state [5], increase T_c of superconductors (T_c of copper oxides is raised to 164 K at 31 GPa) [6], etc. To note, superconductivity under pressure has been extended to most elements of periodic table.

Back in the year 1935, Wigner and Huntington theoretically predicted that solid hydrogen would be metallized at high pressure, that is metallic hydrogen [7], which is believed to be a room-temperature superconductor [8]. Therefore, searching for metallic phase of solid hydrogen becomes a very important topic in physics. There are so many experimental research works on the hydrogen under high pressures. But these works reveal that the metallization of hydrogen is very difficult. Up to date, there is no experimental evidence for the predicted metallic state in the pressure range up to 388 GPa [9]. One of the important topics is how to reduce the metallic pressure of hydrogen system. In 2004, Aschroft [10] proposed a great idea that hydrogen-rich materials can be metallized at much lower pressures due to 'chemical pre-compression'. Because these materials are dominated by hydrogen elements, which can provide high phonon frequencies and strong electron–phonon coupling (EPC), high temperature superconductivity can be found after metallization. Therefore, they are considered as good candidates to search for high T_c superconductors within the reach of the experimental diamond anvil cell (DAC).

Based on this idea, scientists began to search for likely the high-temperature superconductors in hydrogen-rich materials. Because there are some difficulties in the experimental studies of the metallization and superconductivity of hydrogen-rich materials under high pressure, theoretical research works have been at the forefront of this field and made outstanding contributions. The carbon group hydrides with highest content of hydrogen in naturally existed hydrides were first widely studied. Theoretical investigations revealed that silane (SiH_4), germane (GeH_4), stannane (SnH_4), and disilane (Si_2H_6) are metallized at much lower pressure than pure hydrogen with high T_c. For example, SiH_4 is predicted to be 20–75 K [11]. These theoretical predictions really excite the research works on the hydrogen-rich systems under high pressures. Then, can the other hydrogen-rich compounds be expected to be potential candidates for high-T_c superconductivity?

Mixed closed-shell systems and H_2 at high pressure can form new H_2-containing van der Waals compounds, such as $SiH_4(H_2)_2$ and $GeH_4(H_2)_2$, which were predicted to be superconductors with high T_c values of 107 K [12] and 90 K [13] at 250 GPa, respectively. Superconductivity was also reported in alkali metal and alkaline-earth metal hydrides KH_6 [14] and CaH_6 [15], where T_c is 82 K at 300 GPa and 235 K at 150 GPa, respectively. However, only a low $T_c \sim 17$ K of silane at 90 and 120 GPa in these hydrides has been observed through experiment [16], though debates remained. Little experimental research has made the studies of hydrogen-rich materials in depression, but the step has never stopped.

Recently, the novel sulfur hydrides H_3S [17,18] with *Im*-3*m* symmetry was predicted theoretically by our group to be a high-temperature superconductor with T_c reaching as high as 191–204 K at 200 GPa. Subsequently, Drozdov *et al.* observed a high $T_c = 203$ K in H_2S sample at 155 GPa based on the resistant transition, isotope effect, and Meissner effect [19]. The observed T_c values and its pressure dependences are close to our theoretical predicted, suggesting that high T_c in H_2S sample mainly comes from H_3S. Moreover, the *Im*-3*m* structure was confirmed experimentally by synchrotron X-ray diffraction (XRD) more recently [20]. In addition, Mazin specially emphasizes [21] 'this is the first time that a previously unknown material predicted to be a high-temperature superconductor has been experimentally confirmed to be one.'

The discovery of $T_c \sim 200$ K at high pressure in sulfur hydrides by theoretical prediction and experimental measurement reveals that high-T_c in hydrogen-rich materials indeed can be achieved. Therefore, many theoretical predicted stable hydrogen-rich materials are potential candidates for high-temperature superconductors. This review is organized as a systematic summary of the superconducting behavior of the stable hydrides. Beginning from alkali metal hydrides, and ending with halogen hydrides, we discuss structures, metallization, and superconductivity of hydrogen-rich materials at high pressures.

ALKALI METAL HYDRIDES

Up to now, among the alkali metals (Li, Na, K, Rb, Cs) hydrides, only LiH_n and KH_n ($n > 1$) systems were predicted to be superconductors under pressure [14,22]. Except for LiH_n, linear H_3^- units emerge in alkali metals (Na, K, Rb, Cs) hydrides. Moreover, LiH_2, LiH_6, NaH_3, and NaH_7 have been synthesized experimentally [23,24].

Lithium hydrides

LiH_n ($n = 2$–8) was systematically investigated under high pressure in theory [25]. LiH_2 with *P*4/*mbm* symmetry is energetically stable relative to LiH and H_2 at ∼120 GPa, which contains two types of hydrogen: H^- and H_2 units. LiH_6 (space group *R*-3*m*) has the lowest enthalpy of formation above 150 GPa, and it possesses Li and H_2 units. By analyzing the density of states (DOS) for LiH_2 and LiH_6, both of them are insulators at 0 GPa and metalize at 100 GPa. However, the metallization nature of LiH_2 and LiH_6 is different. For the former, pressure-induced band-gap closed between the H^- ('impurity donor band') and H_2 $\sigma_u{}^*$ bands, while for the latter, electron transfers from Li to H_2 $\sigma_u{}^*$ levels. For LiH_8 with *I*422 symmetry, its stable pressure range is 100–200 GPa. The superconductivity of three stoichiometries (LiH_2, LiH_6, and LiH_8) was extensively studied in another theoretical work [22]. LiH_2 is not a superconductor, while LiH_6 and LiH_8 are superconductors. The critical temperatures (T_c) for LiH_6 and LiH_8 are 38 K (150 GPa) and 31 K (100 GPa), respectively, which are mostly due to the intermolecular vibrations of H_2 units. And the T_c of LiH_6 increases with increasing pressure, while the value of T_c for LiH_8 keeps almost no change. The theoretical prediction promotes people to synthesize the lithium hydrides in experiment. In 2012, Howie *et al.* synthesized LiH at 50 MPa, but LiH_x ($x > 1$) was not found [26]. Recently, LiH_2 and LiH_6 were observed above 130 GPa at 300 K. However, when pressure is up to 215 GPa, they both kept insulating [23]. There are some differences in metallization between experiment and theory. Therefore, more research works are needed to study the Li-H system at high pressure.

Sodium hydrides

It was theoretically reported that NaH_n $(n > 1)$ can be stable under pressure [27]. With respect to Li, the ionization potentials of Na is lower, results in that NaH_n can be synthesized at lower pressure than LiH_n. At ∼25 GPa, the NaH_9 becomes thermodynamically stable. Moreover, the phase $Cmc2_1$-NaH_9 adopts H^- and H_2 units and its metallization occurs at 250 GPa. For NaH_7 and NaH_{11}, their stable pressure ranges are 25–100 and 25–150 GPa, respectively. The metallization mechanism and structures between odd and even NaH_n are different. By comparing, the odd NaH_n possesses H^- and H_2 units, and the Na-p deters their metallization, although some can metalize. But the even NaH_n only contains H_2 units, and the H_2 $\sigma_u{}^*$ bands are partially filled by Na-s elections which induce metallic behavior. After a few years, it is reported that NaH_3 and NaH_7 can be synthesized in a laser-heated DAC above 40 GPa and 2000 K [24]. Furthermore, $H_3{}^-$ units were found in NaH_7.

Potassium hydrides

KH_6 was predicted energetically stable above 70 GPa by our group, which possesses two-layered structures $C2/m$ and $C2/c$ [14], as shown in Fig. 1. The former owns H_2 and H_3 units, forming a 1D network. The latter only contains H_2 units, and its arrangements of H atoms are similar to that of solid hydrogen (*Cmca* phase). For $C2/m$, it metalizes at 145 GPa, while $C2/c$ keeps metallic all the time that is a 1D conductor attributed to hydrogen-bonded network. Based on the BCS theory, the calculation showed that the EPC parameter λ and T_c for $C2/c$ reach 0.91 and 58.66–69.84 K at 166 GPa. By further analysis, the potassium atom vibration makes mainly contribution to λ. In addition, $C2/c$ has a negative pressure dependence of T_c in the pressure range from 166 to 300 GPa. In the same year, another group also studied the KH_n $(n > 1)$ under pressure by first-principles calculation [28]. The KH_5 consists of $H_3{}^-$ molecules which become stable at 3 GPa, and it keeps the lowest enthalpy and remains insulator in the studied pressure range. But some metastable phases exhibit metallic properties.

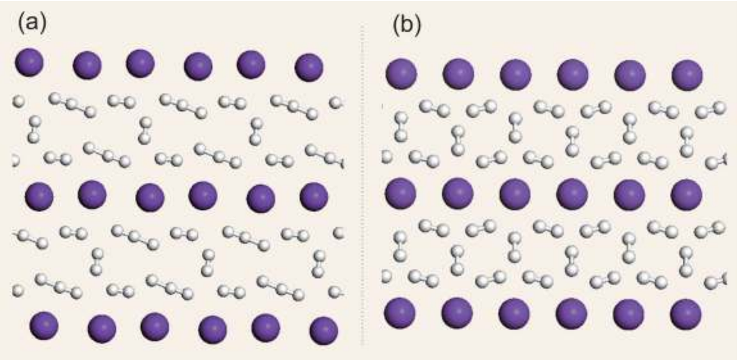

Figure 1. The structures of KH_6 with space group (a) $C2/m$ at 100 GPa and (b) $C2/c$ at 166 GPa [14]. Copyright 2012 American Physical Society.

Rubidium hydrides and cesium hydrides

Rubidium hydrides and cesium hydrides were also studied under pressure [29,30]. For RbH_n $(n > 1)$, some species begin to stabilize at 2 GPa, which contain Rb^+, H_2 and linear $H_3{}^-$ units [29]. Below 100 GPa, two compounds RbH_9 (*Pm*) and RbH_5 (*Cmcm*) are most preferred. RbH_3 is stable above 100 GPa consisting of Rb^+ and $H_3{}^-$. While for RbH_6, the polymeric chains $(H_3{}^-)_\infty$ emerge. Moreover, RbH_3 and RbH_6 are good metals. CsH_n $(n > 1)$ are similar to RbH_n, which become stable at 2 GPa and also possess $H_3{}^-$ units [30]. The compound CsH_3 is preferred in the pressure range of 30 to 200 GPa, while CsH_7 is stable up to 150 GPa. Meanwhile, the author indicated that the metallic phases *Cmmm* and *Cmma* of CsH_3 are attributed to the hydrogen formation.

ALKALINE-EARTH METAL HYDRIDES

For the alkaline-earth metal (Be, Mg, Ca, Ba, and Sr) hydrides, except for SrH_n $(n > 2)$, they are predicted to have high T_c. Especially, the T_c of CaH_6 reaches 220–235 K (150 GPa), which is mostly due to the 'H_4' units [15]. Unfortunately, there is no experimental study up to now.

Beryllium hydrides

Beryllium hydrides have been extensively explored by first-principles calculation. Except the well-known BeH_2, no stoichiometry was found to be thermodynamically stable up to 400 GPa [31,32]. Then, the structures and properties of BeH_2 at high pressure were studied [32,33]. The phase transition sequence at high pressure is $Ibam \rightarrow P\text{-}3m1 \rightarrow R\text{-}3m \rightarrow Cmcm \rightarrow P4/nmm$. The first three phases are insulator and the last two phases are metallic. Moreover, the T_c of metallic *Cmcm* and $P4/nmm$ phases were calculated with 32–44 and 46–62 K at 250 and 400 GPa, respectively. For both phases, the tendency of T_c with pressure is first increased and then decreased.

Magnesium hydrides

Magnesium hydrides under pressure were theoretically searched [34]. MgH_4, MgH_{12}, and MgH_{16}

were found to have lower enthalpy than MgH_2 and H_2 at 92, 122, and 117 GPa, respectively. MgH_4 possesses H^-, H_2, and Mg^{2+}, while $MgH_{12,16}$ adopts $H_2{}^{\delta-}$. The metallic phases *Cmcm*-MgH_4 and *R*3-MgH_{12} show superconductivity with T_c of 29–37 and 47–60 K at 100 and 140 GPa, respectively. Although they both have comparative EPC λ, the average logarithmic frequency of MgH_{12} is larger than that of MgH_4. Therefore, the T_c value of MgH_{12} is higher than that of MgH_4.

Calcium hydrides

Recent theoretical work indicated that by compression, three stoichiometries CaH_4, CaH_6, and CaH_{12} become energetically stable [15]. In addition, the formation of hydrogen in CaH_4, CaH_6, and CaH_{12} is different, which is present for H atoms and H_2 units, H_4 units, and only H_2 units, respectively. Owing to the exotic 'H_4' units which are susceptible to a Jahn-Teller distortion, the electronic property, the bonding feature, and superconductivity of CaH_6 were investigated. And the covalent bond in H_4 units is obvious by calculated electron localization function (ELF). The 'H_4' contributes more to EPC. Further calculation shows that the λ and T_c are 2.69 and 220–235 K at 150 GPa, respectively. And the T_c shows a decreasing trend with pressure. Although CaH_6 has been predicted as a good superconductor, it has not been observed in experiment.

Strontium hydrides and barium hydrides

Sr-H and Ba-H systems at high pressure were investigated theoretically in detail. For Sr-H system, SrH_4, SrH_6, SrH_{10}, and SrH_{12} become thermodynamically stable under compression [35,36]. While for Ba-H system, pressure induced BaH_6, BaH_8, and BaH_{12} are stable, in which the hydrogen sublattices are H^-, $H_3{}^-$ and H_2 units [31]. In addition, *P*4/*mmm*-BaH_6 possesses lower enthalpy and the calculated T_c is 30–38 K at 100 GPa.

BORON GROUP HYDRIDES

Except for thallium element, the other boron group hydrides have been intensively studied. For boron hydrides, the estimated T_c of B_2H_6 and BH are 125 and 14.1–21.4 K at high pressure [37,38]. There are an amount of research works on AlH_3, however, the argument about its superconductivity is existent. GaH_3 is stable above 160 GPa, and its calculated T_c reaches 86 K [39]. For indium hydrides, the T_c of *R*-3-InH_3 and *P*2$_1$/*m*-InH_5 at 200 and 150 GPa are 34.1–40.5 and 22.4–27.1 K, respectively [40].

Boron hydrides

For boron hydrides, the well-known stoichiometry is diborane B_2H_6. But theoretical prediction revealed that B_2H_6 ($P2_1/c$) became unstable and decomposed into BH (*Ibam*) and H_2 at 153 GPa [37]. Moreover, BH can coexist with B_2H_6 between 50 and 153 GPa. It is interesting that B_2H_6 re-stabilizes again with *Pbcn* symmetry beyond 350 GPa, and the calculated T_c is 125 K at 360 GPa [38]. For BH, it has two structures, a semimetallic *Ibam* and a metallic *P*6/*mmm*. The calculated T_c of *P*6/*mmm* reaches 14.1–21.4 K at 175 GPa and decreases with increasing pressure.

Aluminium hydrides

Aluminum hydride (AlH_3) at high pressure gains people's attention and has been widely explored both in theory and experiment. In 2007, the phase transition at high pressure was given as *R*-3*c* (phase I) → *Pnma* (phase II) → *Pm*-3*n* (phase III) at 24 and 73 GPa, respectively. Moreover, both *R*-3*c* and *Pnma* are insulators, whereas *Pm*-3*n* becomes metallic [41]. The calculated T_c of *Pm*-3*n* was 24 K at 110 GPa, but its superconductivity was not observed in experiment [42]. Later, a theoretical work provided an explanation about why the experimental and theoretical data on T_c of AlH_3 is distinct [43]. Considering anharmonic self-energy, the calculated value of T_c reduces to as low as 2 K. Therefore, the distinction between experimental and theoretical data is attributed to the anharmonicity that suppresses the EPC parameter. In addition, the metallic phase *Pm*-3*n* can be stabilized at ambient condition once a finite electronic temperature is considered [44].

AlH_3 (H_2) was also investigated from 25 to 300 GPa in theory by our group [45]. It undergoes two phase transitions, from insulating *P*1 to semiconductor *P*-1, then to metallic *P*2$_1$/*m* at 75 and 250 GPa, respectively. In addition, H_2 units were found in *P*2$_1$/*m* phase. The calculated T_c of metallic *P*2$_1$/*m* is 132–146 K at 250 GPa, having a large λ of 1.625. It is noted that the total λ is mostly from mediate modes, while contribution of H_2 is little.

Gallium hydrides and indium hydrides

As we know, unlikely BH_3 and AlH_3, GaH_3 and InH_3 are thermodynamically unstable at ambient conditions. Up to now, it is theoretically reported that GaH_3 with *Pm*-3*n* symmetry is thermodynamically stable relative to Ga and H_2 above 160 GPa [39]. The calculated T_c reaches 86 K at 160 GPa, and H atoms play an important role in superconductivity.

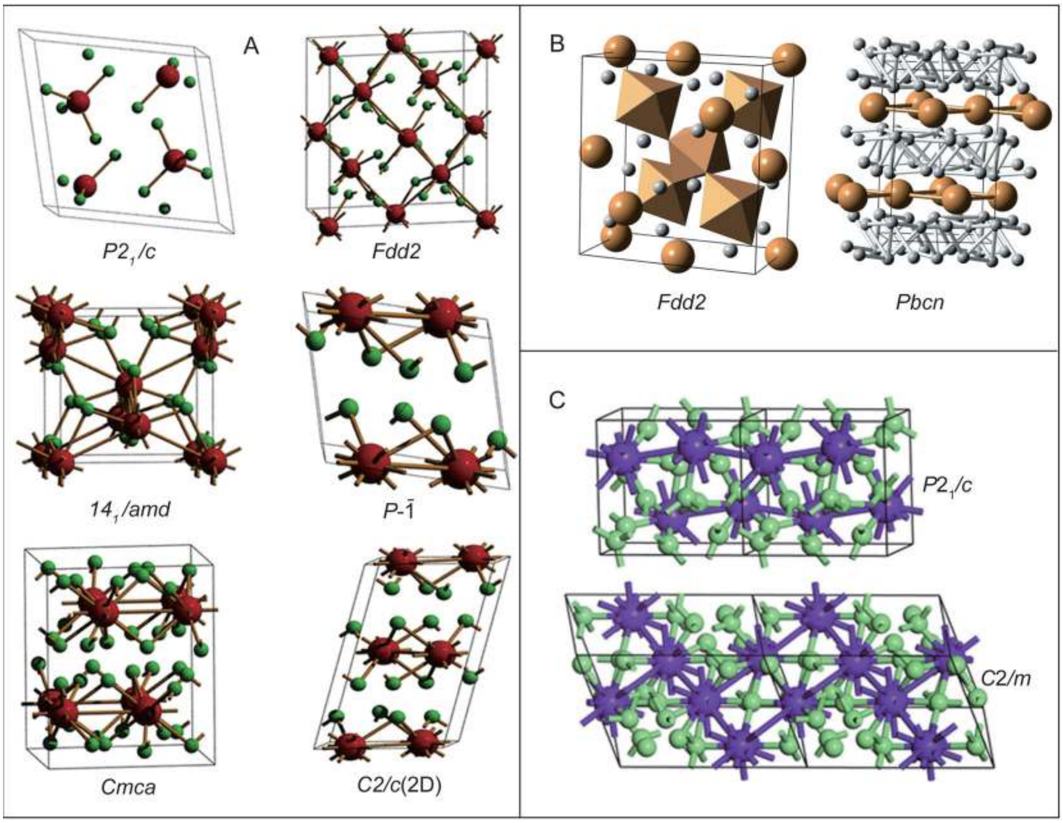

Figure 2. The selected high-pressure crystal structures of silane. Adapted from [11,53,55]. Copyright 2008 and 2009 American Physical Society.

The theoretical study of indium hydrides in a wide pressure range of 0–300 GPa was performed by our group [40]. Two stoichiometries InH_3 and InH_5 were found to be stable by compressing. The InH_5 can be synthesized at 120 GPa by $2In + 5H_2 \rightarrow 2InH_5$. And then the decomposition happened by $InH_5 \rightarrow InH_3 + H_2$, which demonstrated that InH_3 becomes favorite stoichiometry till 300 GPa. The lowest-enthalpy stable phases of InH_3 and InH_5 are R-3 and $P2_1/m$ symmetry, respectively. And they both possess H_2 or H_3 units. In addition, electrons move from In atoms to H atoms by Bader analysis. The EPC calculations show that the metallic R-3-InH_3 and $P2_1/m$-InH_5 have a large λ of 0.92 and 0.85, resulting in the estimated T_c of 34.1–40.5 K at 200 GPa and 22.4–27.1 K at 150 GPa, respectively.

CARBON GROUP HYDRIDES

The concept of ‘chemical pre-compression’ first appeared by doping the IVa group elements to hydrogen [10] and the hydrides with carbon group elements were widely studied even now. For the first element with the lowest mass, CH_4, the results were not very satisfactory [46]. The metallization of CH_4 did not occur up to 520 GPa by first-principle calculation [47]. But many works suggested that the other carbon group (Si, Ge, Sn, and Pd) hydrides may realize the metallization and become superconductors under pressure.

Silicon hydrides

For silane (SiH_4), a great deal of theoretical and experimental works [11,16,48–55] were carried out to explore the crystal structures, metallization, and superconductivity under high pressure. It is found that there are at least 10 high-pressure phases ($Pman$, $C2/c$, $P6_3$, P-1, $Cmca$, $P4/nbm$, $Pbcn$, P-3, $P2_1/c$, and $C2/m$) of SiH_4 in the pressure range of 50 and 606 GPa, as shown in Fig. 2. Among them, one phase ($P6_3$) was found in the experiment and others were from the theoretical prediction [16]. All of these structures could achieve metallization and exhibit superconductivity with T_c of 16–166 K at lower pressure than pure hydrogen. Except for extreme pressures (383–606 GPa) [55], there still exist controversies on the most stable structures of SiH_4 at the corresponding pressures. Specifically, Degtyareva *et al.* explained that the metallization of $P6_3$-SiH_4 might be due to the decomposition of SiH_4 and the reaction between H and the environment materials like Pt or Re [56].

Based on the above explorations, our group performed more extensive study on disilane (Si_2H_6) [57], and found three crystalline structures *P*-1 (135–275 GPa), *Pm*-3*m* (275–300 GPa), and *C*2/*c* (300–400 GPa). Furthermore, the estimated T_c of *P*-1 at 200 GPa, *Pm*-3*m* at 275 GPa, *C*2/*c* at 300 GPa is 92, 153, 42 K, respectively. Afterwards, Flores-Livas *et al.* proposed a new metallic phase of disilane with *Cmcm* symmetry [58] at 190–280 GPa with $T_c \sim 13$ K at 220 GPa.

Besides the silicon hydrides naturally existed, a new molecular compound $SiH_4(H_2)_2$ was observed from silane-hydrogen mixtures at ∼6.8 GPa by XRD and Raman experiments [59,60]. And a possible group space *F*-43*m* [59] of $SiH_4(H_2)_2$ was provided. Later, theoretical works [61–64] were attempted to study structures and superconductivity at high pressure. They proposed three phases *F*-43*m* [61], *I*-4*m*2 [62–64], *Pmn*2$_1$ [63] at ∼6.8 GPa, and two new metallic phases with *P*1 (125 GPa) [64] and *Ccca* (248 GPa) [12] at higher pressures. Furthermore, calculation showed that *Ccca* phase possesses a T_c of 98–107 K at 250 GPa [12].

Germanium hydrides

The research works on GeH_4 were mainly concentrated on theoretical predictions [65–67]. It is found that there are at least seven phases (*I*4/*mmm*, *P*-43*m*, *I*-42*m*, *Pman*, *C*2/*m*, *Ama*2, and *C*2/*c*) in the pressure range of 0 and 500 GPa and all phase can become metal with the increasing pressure. Moreover, three metallic phases (*C*2/*m*, *Ama*2, and *C*2/*c*) exhibited superconductivity with T_c of 40–84 K at high pressures. In addition, our group study revealed that GeH_3 with *Cccm* symmetry is stable above 280 GPa, and has a T_c of 80 K at 300 GPa [68]. A new molecular compound $GeH_4(H_2)_2$ can be synthetized at 7.5 GPa by experiment [69]. Furthermore, the metallic phase *P*2$_1$/*c* of $GeH_4(H_2)_2$ was proposed to have the T_c of 76–90 K at 250 GPa [13].

Stannum hydrides

For SnH_4, Tse, Yao and Tanaka proposed a *P*6/*mmm* structure with $T_c \sim 80$ K at 120 GPa [70]. They claimed that soft phonons and Kohn anomalies play an important role in improving the electron–phonon interaction. Later, Gao *et al.* [71] predicted two metallic phase of SnH_4 with *Ama*2 symmetry at 96–180 GPa and *P*6$_3$/*mmc* symmetry above 180 GPa. *Ama*2 phase has a T_c of 15–22 K at 120 GPa and the T_c in *P*6$_3$/*mmc* is 52–62 K at 200 GPa.

Plumbum hydrides

For PbH_4, two-layered metallic phases *Imma* (132–296 GPa) and *Ibam* (above 296 GPa) were predicted [72]. In both phase, electrons near Fermi level are analogous with free electrons which exhibit not only metallic but also diffusive or liquid-like properties. Another theoretical work explored the high-pressure crystal structure, metallic and superconductivity of $PbH_4(H_2)_2$ [73]. Their calculations revealed that the $PbH_4(H_2)_2$ with *C*2/*m* symmetry could become metal above 133 GPa and exhibit T_c of 107 K at 230 GPa.

For carbon group hydrides, some potential regular patterns can be summarized. First, H_2 units gradually prefer to appear in MH_4 (Ge, Sn and Pb) with the increasing radius of impurity elements (Si, Ge, Sn and Pb). Second, the EPC parameter in SiH_4 is mainly contributed by H-Si-H vibration. While in GeH_4, SnH_4, $GeH_4(H_2)_2$, and $SnH_4(H_2)_2$, the EPC parameter are mainly derived from the intermediate frequency region, mostly corresponding to the vibration of H-M-H or the interaction of M and H_2 units. Third, for $MH_4(H_2)_2$ (Ge, Sn and Pb) systems, with the increasing pressure, charges transform from intra-molecular of MH_4 units to two sites: one is H_2 units, and the other is the interstitial between MH_4 and H_2 units. Besides, their superconducting transition temperatures are always higher than the corresponding MH_4, which means the additive hydrogen plays an important role in improving the superconductivity of hydrides.

PNICTOGEN HYDRIDES

As the pnictogen element, NH_3 have been studied widely, but they have difficulty in achieving metallization under high pressure. Unluckily, the hydrides of phosphorus, arsenic, and antimony are seldom to be studied under high pressure. The H_3S-*Im*-3*m* with a high superconducting transition temperature values of 191–204 K at 200 GPa predicted by our group [17] and proved by Drozdov *et al.* [19] has been broadly accepted. Later, our group executed a series of systemic research works to explore the high pressure crystal structures and superconductivity in antimony and bismuth hydrides [74,75]. We found that T_c of SbH_4 at 150 GPa reaches 118 K and T_c of BiH_5 at 300 GPa reaches 119 K.

Phosphorus hydrides

More recently, Drozdov, Eremets and Troyan performed resistivity measurements on covalent phosphine (PH_3) samples which metallize at 40 GPa, show superconductivity at 83 GPa with $T_c \sim 30$ K and the maximum T_c reaches 103 K at ∼207 GPa [76]. But the exact composition and crystal structure of the superconducting phase are not determined. Subsequently, density functional theory calculations show that PH_2 [77] with $C2/m$ symmetry consisting of two formula units in the primitive cell could be a candidate hydride with $T_c \sim 82$ K at 200 GPa. But other theoretical calculations show that all the phosphorus hydrides are thermodynamically unstable with respect to P and H_2 in the pressure range 100–300 GPa [78,79]. The calculated T_c of PH_2 with $I4/mmm$ symmetry is 40 K at 100 GPa, and reaches a maximum value of 78 K at 220 GPa. In addition, the T_c dependence on pressure of PH is in agreement with experiment. Although the calculated T_c of PH, PH_2, and PH_3 with respect to pressure are comparable to experiments, the superconducting phase remains unclear.

Arsenic hydrides and antimony hydrides

For arsenic hydrides, there is only AsH and AsH_8 stable above 300 GPa and AsH_8 is predicted to exhibit T_c values of ∼150 K above 350 GPa [80]. The metallic SbH_4-$P6_3/mmc$ phase with nontrivial binding stable above 127 GPa was uncovered to have the most negative enthalpy among all of the researched antimony hydrides [74]. In $P6_3/mmc$-SbH_4, there exists unequivalent hydrogen marked H1 and H2 which occupy on $4e$ and $4f$ sites. One kind of hydrogen (H1) is bound with strong covalent interaction to form H_2 units and the other kind of hydrogen (H2) binds with the nearest Sb atom to form weak covalent bonds. Startlingly, the apparent charge localizes between Sb and H2 atoms when the isosurface value of 0.7 is selected but the value of ELF fades in 0.75, implying the nearest Sb and H2 atoms form startling weak polar covalent bonds. Besides, the T_c of 118 K was obtained in $P6_3/mmc$-SbH_4 at 150 GPa. With the increasing pressure, T_c decreases (118 K at 150 GPa and 86 K at 300 GPa for $\mu^* = 0.10$) at a descendant gradient (dT_c/dP) of −0.21 K/GPa, which means T_c has only a weak dependence on pressure. Subsequently, the same high-symmetry structure of SbH_4 was found by using two different structural search techniques [80]. Moreover, they obtained the T_c of 102 K at 150 GPa, which confirms our theoretical prediction.

Bismuth hydrides

For BiH_n ($n = 1$–6), except for BiH_3, all stoichiometries are stable at high pressure [75]. The remarkable structural feature is the emergence of H_2 units in BiH_2, BiH_4, and BiH_6. BiH_5 adopts a startling layered structure intercalated by H_2 and the linear H_3 units. The ionic bonding feature in Bi-H system is quite different from the same group covalent hydride of SbH_4, and the discrepancy of bonding feature depends on the existing form of hydrogen atoms and individual crystalline structures. In SbH_4, except for H_2 units, it also contains Sb-H weak interaction. However, except for BiH, only H_2 or H_3 units were found in Bi-H system and no excrescent hydrogen can bind with Bi atoms. On the other hand, the elemental nature could determine the discrepancy. In pnictogen group, nitrogen (N) and phosphorus (P) are nonmetal, and arsenic (As) and antimony (Sb) are regarded as semimetal, while bismuth (Bi) is the sole ‘real metal’. Compared with other pnictogen elements, bismuth has the heaviest atomic mass and the weakest electronegativity. In Bi-H system, H atoms may have a stronger ability in attracting electrons than Bi and then form the ionic bonding. Furthermore, the calculated T_c of BiH, BiH_2, BH_4, BiH_5, and BiH_6 at 300 GPa are 20, 65, 75, 119, and 113 K, respectively, which indicates all these stable bismuth hydrides are potential high-temperature superconductors. It also can be seen that the T_c increases with the increasing hydrogen content with the maximum value of 119 K in BiH_5. The results of Bi-H system verify the idea that hydrogen content has a great influence on the superconducting transition temperature. In addition, the T_c of BiH and BiH_4 decrease with the increasing pressure, while the T_c increases with the increasing pressure in BiH_2, BiH_5, and BiH_6.

CHALCOGEN HYDRIDES

As the lightest chalcogen hydrides, H_2O has a rich phase diagram: amorphous, hydrogen bond symmetry, ionic phase and so on [81]. Unfortunately, it has difficulty in achieving metallization up to 2 TPa [82]. For other chalcogen hydrides, they show metallic properties and high-temperature superconductivity at lower pressure; especially for new sulfur trihydrides H_3S, it sets a record high critical temperature of 200 K [17–19].

Sulfur hydrides

In 1990s, the structures and molecular dissociation of solid H_2S at high pressure have been studied extensively, but this remains controversial. In 1997, infrared-absorption spectral measurement at room temperature showed that H_2S molecules dissociate and metalize at 46 and 96 GPa, respectively [83]. In 2010, our group theoretically predicted that protons are delocalized and can move back and forth along the S–S separation in phase V of H_2S [84]. It is

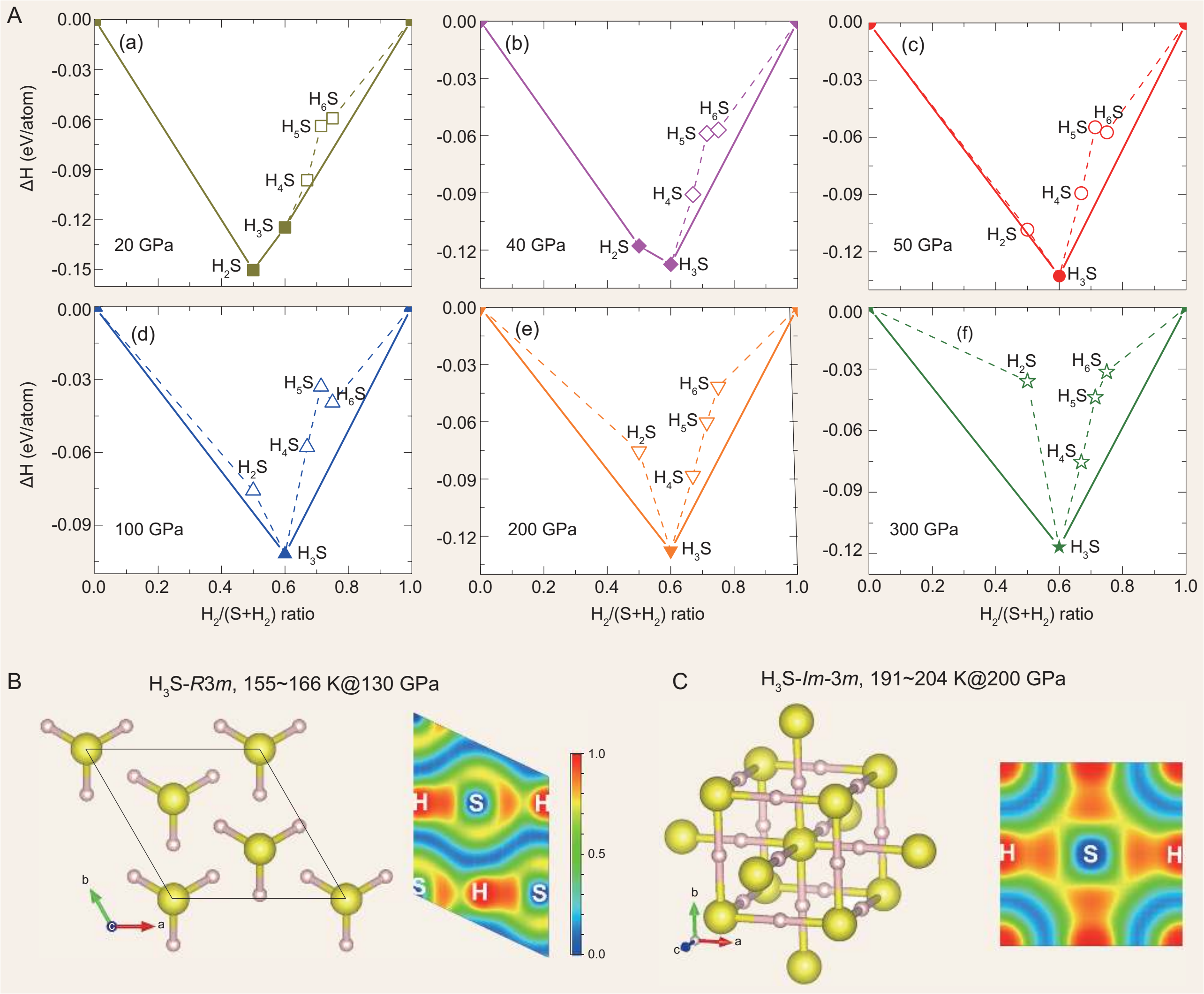

Figure 3. (A) Predicted formation enthalpies of H_nS with respect to decomposition into S and H_2 under pressure [18]. Dashed lines connect data points, and solid lines denote the convex hull. Copyright 2015 American Physical Society. (B) Crystal structures of H_3S-*R*3*m* and its corresponding ELF [17]. (C) Crystal structures of H_3S-*Im*-3*m* and its corresponding ELF [17].

indicating that the decomposition of H_2S under high pressure is not simple. In 2014, it was theoretically predicted that H_2S cannot decompose into sulfur and hydrogen up to 200 GPa [85]. Moreover, two metallic phase *P*-1 and *Cmca* were proposed with the highest $T_c \sim 80$ K at 160 GPa.

In 2011, it is reported that mixing H_2S and H_2 can form a new compound $(H_2S)_2H_2$ (H_3S, the stoichiometric ratio of H and S atoms is 3:1) near 3.5 GPa [86]. Unfortunately, the highest pressure in this study is 30 GPa. In 2014, we have extensively explored the high-pressure structures and superconductivity of H_3S through *ab initio* calculations [17]. The low pressure crystal structure with *P*1 symmetry (below 37 GPa) has been determined. Moreover, the XRD, Raman, and equation of states for *P*1 are in excellent agreement with experimental results. Furthermore, three new high-pressure phases were firstly proposed: orthorhombic *Cccm* (37–111 GPa), hexagonal *R*3*m* (111–180 GPa), cubic *Im*-3*m* (180–300 GPa). Interestingly, there are H_2 units in insulating phase *P*1 and *Cccm*, whereas H_2 units disappear in metallic phases *R*3*m* and *Im*-3*m*, and hydrogen atoms cooperating with sulfur atoms form strong covalent bonding, as shown in Fig. 3. Further EPC calculations predict that the T_c of the *R*3*m* phase at 130 GPa is 155–166 K. Remarkably, we predicted the T_c of the *Im*-3*m* phase to achieve 191–204 K at 200 GPa for the first time, reaching an order of 200 K. In addition, T_c increases with increasing pressure in the *R*3*m* phase (135–145 K at 110 GPa and 165–175 K at 150 GPa), whereas T_c decreases nearly linearly with increasing pressure in the *Im*-3*m* phase (184–200 K at 250 GPa

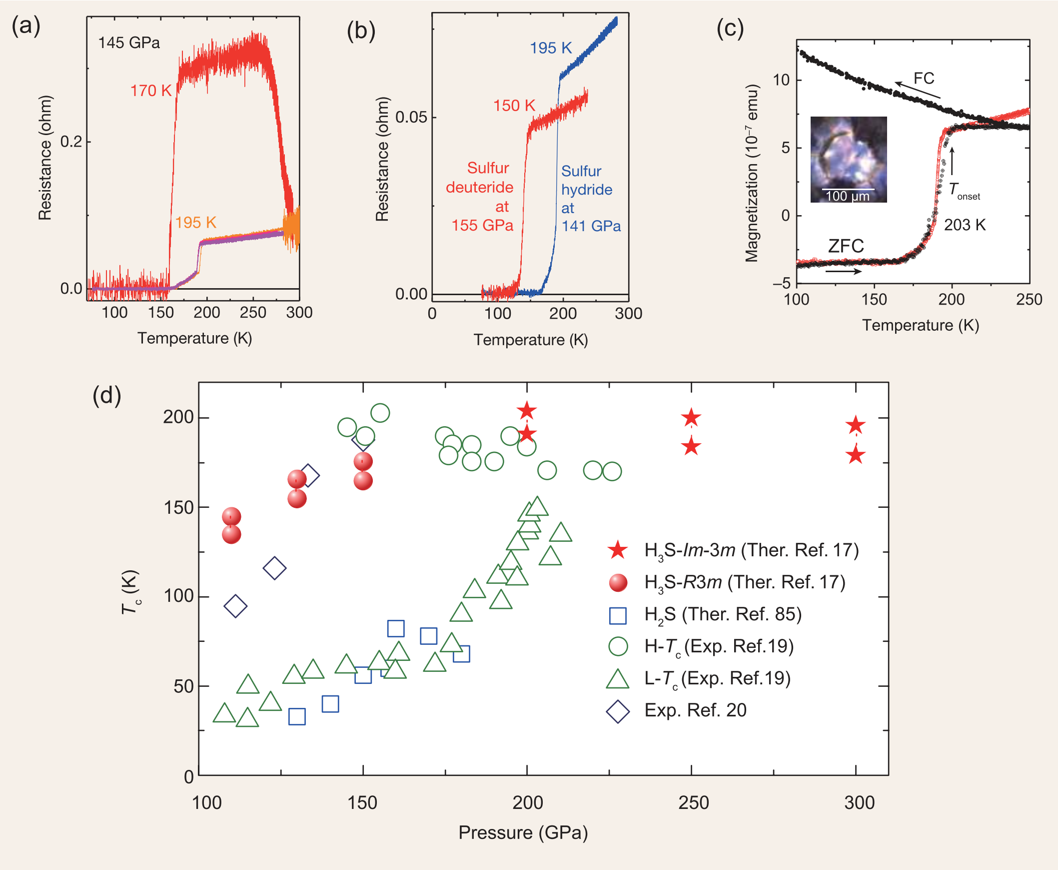

Figure 4. (a) Changes of resistance and T_c of sulfur hydride with temperature at constant pressure—the annealing process. (b) Typical superconductive steps for sulfur hydride (blue trace) and sulfur deuteride (red trace). (c) Temperature dependence of the magnetization of sulfur hydride at a pressure of 155 GPa in zero-field cooled (ZFC) and 20 Oe field cooled (FC) modes (black circles). Adapted from [19]. Copyright 2015 Nature Publishing Group. (d) Dependence of T_c on pressure for experimental and theoretical results [17,19,20,85].

and 179–196 K at 300 GPa). Further analysis shows that H atoms play a significant role in superconductivity of H_3S. In addition, we performed the high-pressure stability of different stoichiometric H_nS ($n > 1$) using *ab initio* calculations [18] and determined two main ways to form H_3S crystal: $3H_2S \rightarrow 2H_3S + S$, $2H_2S + H_2 \rightarrow 2H_3S$, as depicted in Fig. 3. That is, H_3S can be obtained by directly compressing pure H_2S above 43 GPa [18] or mixing H_2S and H_2 at lower pressure [18,86]. The other theoretical research works also confirmed our results in succession [87,88]. Excitingly, superconductivity in an H_2S sample with high T_c = 203 K above 155 GPa has been observed based on the resistant transition, isotope effect and Meissner effect [19], as shown in Fig. 4. Moreover, Shimizu *et al.* in cooperation with Eremets further confirm that the H_2S decomposes H_3S and S at high pressure by XRD measurements [20]. In addition, they also confirm that the superconducting (SC) phase is mostly in good agreement with our theoretically predicted body-centered cubic structure [17].

There is a widespread consensus that the superconducting samples are composed of sulfur trihydride (H_3S) *Im*-3*m* phase proposed by our group and is considered to be conventional in nature. Therefore, there are a lot of theoretical research works using the *Im*-3*m* structure to study the superconducting mechanism of H_3S by analysis of the electronic structure and bonding characteristics. Bernstein *et al.* underlined that the high-temperature superconductivity of H_3S is attributed to strong covalent bonds giving rise to large EPCs [87], which is similar to the MgB_2. In addition, a more detailed study on Van Hove singularity of H_3S proposes that increasing the electron DOS near the Fermi surface will increase the superconducting transition temperature [89]. Heil and Boeri constructed hypothetical alchemical atoms by partially replacing sulfur with chalcogen group element and showed that the critical temperatures of H_3S could be improved by increasing the ionic character of the relevant bonds [90]. Besides the substitution of S by elements in the same main group, further substitutions by phosphorus and halogen group element, and in the optimized case of $H_3S_{0.925}P_{0.075}$, the T_c may reach a record high value of 280 K at 250 GPa [91].

Selenium hydrides

For selenium hydrides, H_3Se is stable above 166 GPa which possess *Im*-3*m* symmetry isostructural to that of H_3S [92]. But the predicted T_c of 116 K at 200 GPa is lower than that of H_3S, which is mainly due to the reduced λ. In addition, the other selenium hydrides, the Se-rich HSe_2 (*C*2/*m*), and HSe (*P*4/*nmm*) are stable above 124 and 249 GPa, respectively.

Tellurium hydride

For H-Te system, H_4Te, H_5Te_2, HTe, and HTe_2 were found to be stable above 140 GPa [93]. H_4Te with *P*6/*mmm* symmetry is stable above 162 GPa, and then transforms to *R*-3*m* at 234 GPa, and both phases contain H_2 units. H_5Te_2 adopts *C*2/*m* symmetry with intriguing linear H_3 units. For HTe, *P*4/*nmm* phase is stable above 140 GPa which is isostructural to HSe. Then it transforms to $P6_3/mmc$ phase near 286 GPa. The T_c for H_4Te, H_5Te_2, and HTe are estimated to be 99, 58, and 19 K at 200 GPa, respectively.

Polonium hydrides

For H-Po system, several stoichiometries (PoH, PoH_2, PoH_4, and PoH_6) are stable with respect to Po and H_2 under pressure [94]. Moreover, except PoH, PoH_2, PoH_4, and PoH_6 contain H_2 units. PoH adopts $P6_3/mmc$ symmetry and it is isostructural to HTe. The T_c of PoH_4 (space group *C*2/*c*) is predicted to be 47 K at 200 GPa.

HALOGEN HYDRIDES

The consensus for HX (X = F, Cl, Br) is that $Cmc2_1$ phase transforms to hydrogen bond symmetry phase *Cmcm* at high pressure [95–98]. For HI, a complex triclinic phase with *P*1 in a different symmetry appears at low temperatures [98]. Interestingly, triangular $H_3{}^+$ species are unexpectedly found in H_2F, H_3F, H_5F, H_5Cl, and H_5Br above 100 GPa, while there is no $H_3{}^+$ species in H_nI (n = 1–6). With decreasing the electronegativity of halogen, HX (X = F, Cl, Br, and I) becomes unstable and decomposes into other stoichiometries at lower pressure. In addition, the metallization pressure is gradually decreased with decreasing the electronegativity. The electronegativity of bromine is between chlorine and iodine; the structure and stability of H_nBr is not only resemble with H_nCl but also similar with H_nI.

Fluorine and chlorine hydrides

H_nF (n = 1–5) and H_nCl (n = 1–9) have been extensively studied by our group through *ab initio* calculations [99]. The results show that HF is the only stable stoichiometry up to 300 GPa, whereas other stoichiometries $H_{2,3,4,5}F$ are metastable at high pressure. It is interesting that triangular $H_3{}^+$ species are unexpectedly found in stoichiometries H_2F with $[H_3]^+[HF_2]^-$, H_3F with $[H_3]^+[F]^-$, and H_5F with $[H_3]^+[HF_2]^-[H_2]_3$. A perfect equilateral triangle with H–H bond length 0.854 Å is formed in H_5F.

HCl is stable up to 300 GPa with the high pressure phase sequence $Cmc2_1$ → *Cmcm* → *P*-1 → *C*2/*m* [95–97]. And stoichiometries H_2Cl, H_3Cl, H_5Cl, and H_7Cl were found to become stable at high pressure [99–101]. H_2Cl with *C*2/*c* symmetry is stable in a wide pressure range from 12 to 341 GPa, then it transforms to *R*-3*m* phase. H_3Cl adopts three high pressure phases with symmetry *Cc* (12–40 GPa), *C*2/*c* (40–60 GPa), and $P2_12_12_1$ (60–120 GPa). H_5Cl prefers a *Cc* symmetry between 120 and 250 GPa. H_7Cl ($P2_1$ symmetry) with the highest hydrogen content is found to be stable in a narrow pressure range from 70 to 110 GPa. Besides the H-rich compounds, a Cl-rich compound H_4Cl_7 was also found [101]. It possesses two high pressure phase *C*2/*m* (90–278 GPa) and *C*2/*c* (278–445 GPa).

For the hydrogen-rich H-Cl compounds, the stable phases contain covalent HCl zigzag chain which resembles pure HCl of $Cmc2_1$ or *Cmcm* phase and H_2 molecules units. Instead of covalent HCl molecular units, there exists $H_3{}^+$ molecular cation and Cl^- anion in H_5Cl. Importantly, we clearly see the formation process of $H_3{}^+$ through bond length, bond overlap population, ELF, and Bader charge as a function of pressure, as shown in Fig. 5. Moreover, formation of $H_3{}^+$ species is mainly due to charges in hydrogen atoms transfer into chlorine atoms at high pressure. It is also reported that the T_c of HCl- *C*2/*m* at 250 GPa and H_2Cl-*R*-3*m* at 450 GPa are 20 and 45 K, respectively [96,101].

Bromine hydrides

Different from HF and HCl, our calculations show that HBr is unstable above 64 GPa and decomposes into new hydrides H_2Br and Br_2 [102]. In previous experimental research on HBr at high pressure, the Raman spectra of Br_2 molecules were observed after hydrogen-bond symmetrization, but Raman signals

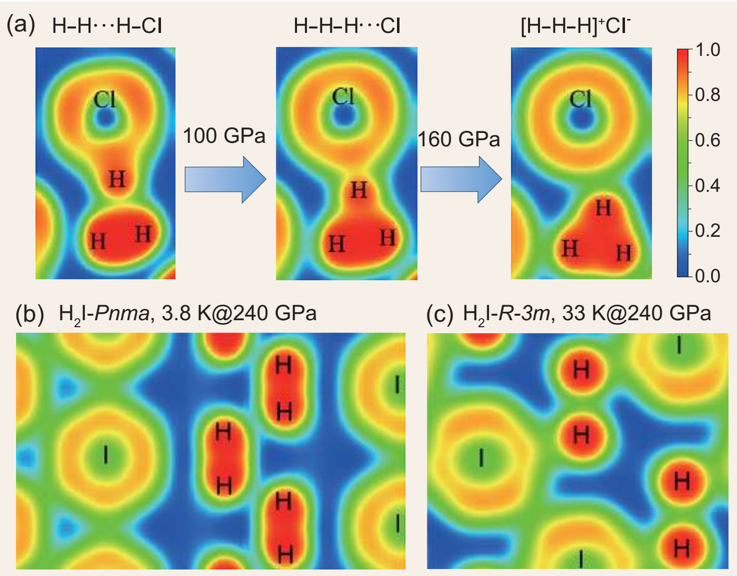

Figure 5. (a) Electron localization function (ELF) maps of H_5Cl-*Cc* with increasing pressure [99]. Copyright 2015 American Chemical Society. (b) ELF maps of H_2I-*Pnma* for (010) plane. (c) ELF maps of H_2I-*R*-3*m* for (110) plane. Adapted from [104] with permission from the PCCP Owner Societies.

of H_2 molecules were not detected [103]. Combining the theoretical calculation results, it is suggested that HBr decompose into H_2Br and Br_2 at high pressure via the reaction $4HBr \rightarrow 2H_2Br + Br_2$. This phenomenon reminds us that H_2S decomposes into new hydrides H_3S and S at high pressure [18].

H_2Br with $C2/c$ symmetry is stable in the pressure range from 30 to 140 GPa. Then, up to 240 GPa, a *Cmcm* phase is formed. H_3Br with $P2_12_12_1$ symmetry can be synthesized via the reaction $HBr + H_2 \rightarrow H_3Br$ above 8 GPa. It transforms into low symmetry *P*-1 phase at about 100 GPa. Different from H-Cl compounds, H_4Br with hexagonal $P6_3/mmc$ structure was observed at 240 GPa. H_5Br contains three high pressure phases with symmetry $C2/c$ (70–100 GPa), *Cc* (100–140 GPa), and $Pmn2_1$ (140–280 GPa). H_7Br with $P2_1/m$ symmetry was found to be stable from 30 to 60 GPa.

For the stable lower pressure phases, they contain covalent HBr zigzag chain which resembles to pure HBr of $Cmc2_1$ or *Cmcm* phase and H_2 molecules units. In the high pressure phase *Cc* and $Pmn2_1$ of H_5Br, they consist of $H_3{}^+$ molecular cation, Cl^- anion, and H_2 molecules units. The structure of H_5Br-*Cc* is very similar to H_5Cl-*Cc*. For H_5Br-$Pmn2_1$ at 140 GPa, H_3 unit forms an approximate equilateral triangle with H–H length of 0.903, 0.903, and 0.911 Å. H_2Br-*Cmcm* consists of monatomic lattices of bromine and H_2 molecules units, which is a good metal. For the case of H_4Br-$P6_3/mmc$, H-Br forms 3D network that traps H_2 molecules arranged in a straight chain, which is also a metal. Further, EPC calculations show that hydrogen-rich H_2Br and H_4Br are superconductors with T_c of 12.1 K and 2.4 K at 240 GPa, respectively.

Iodine hydrides

For HI with the smallest electronegativity of iodine, it decomposes into solids H_2 and I_2 at lower pressure of 6.7 GPa [104]. Different from the other halogen hydrides, there is no $H_3{}^+$ species in hydrogen-rich H_nI ($n = 1$–6). Increasing pressure to 20 GPa, mixed solids H_2 and I_2 can synthetize H_5I with $P222_1$ symmetry, which consist of zigzag rectangular chains built from [I–H–I] units and H_2 molecular units. At about 114 GPa, H_5I decomposes into H_4I ($P6/mmm$) and H_2. In addition, H_2I with *Pnma* is stable in a wide pressure range of 100–246 GPa, then transforms to *R*-3m phase.

In H_4I-$P6/mmm$ and H_2I-*Pnma*, iodine forms a monatomic tube network that traps H_2 molecules units [104]. In the case of H_2I-*R*-3m, iodine monatomic still exists, but H_2 molecular units disappear forming an atomic phase, as depicted in Fig. 5. Further EPC calculations show that the T_c of H_4I-$P6/mmm$ is 17.5 K at 100 GPa [105] and 9.9 K at 120 GPa [104]. In addition, the T_c of *Pnma* and *R*-3*m* phases for H_2I are 3.8 and 33 K at 240 GPa, respectively [104]. Significantly, the T_c of atomic phase *R*-3*m* is increased eight times that of *Pnma*, which is mainly attributed to increment EPC λ, logarithmic average phonon frequency $\omega_{\log}$, and electric DOS values at Fermi level.

CONCLUSIONS AND PROSPECTS

In summary, the 33 classes of main group elements hydrides at high pressure are surveyed above and covered in detail in this review. They exhibit a rich variety stoichiometry and new structures, and show novel superconductivity at high pressure. Above all, the recent discovery of record $T_c \sim 200$ K in sulfur hydrides under high pressure injects fresh energy into the field of searching high temperature superconductor in hydrogen-rich materials. For example, a high $T_c \sim 100$ K of pnictogen hydrides at high pressure was discovered by experimental and theoretical studies. The extensive study on room temperature superconductors in hydrogen-rich materials at high pressure is an exciting long-term research frontier. Finally, more experimental research works are needed to prove the theoretical prediction of novel high-temperature superconductors under high pressure, although experimental challenges are significant.

Table 1. Summary of the maximum superconducting transition temperature of hydrogen-rich materials at high pressures.

Main group hydrides	Hydrides	Structure (stable pressure range GPa)	Maximum T_c (K)	Pressure (GPa)	Reference
Alkali metal	LiH_6	*R-3m* (>140)	38	150	[22,26]
	LiH_8	*I422* (100–200)	31	100	[22,26]
	KH_6	*C2/c* (166–300)	70	166	[14]
Alkaline-earth	BeH_2	*Cmcm* (202–400)	62	400	[32,33]
	MgH_4	*Cmcm* (>92)	37	100	[34]
	MgH_{12}	*R3* (>122)	60	140	[34]
	CaH_6	*Im-3m* (127.7–200)	235	150	[15]
	BaH_6	*P4/mmm* (50–100)	38	100	[31]
Boron group	BH_3	*Pbcn* (350–400)	125	360	[38]
	AlH_5	$P2_1/\mathrm{m}$ (75–250)	146	250	[45]
	GaH_3	*Pm-3n* (160–300)	86	160	[39]
	InH_3	*R-3* (223–300)	40	200	[40]
	InH_5	$P2_1/m$ (120–223)	27	150	[40]
Carbon group	SiH_4	*Pman* (> 96)	166	202	[48]
	SiH_3	*Pm-3m* (275–300)	153	300	[57]
	SiH_8	*Ccca* (24–300)	107	250	[63]
	GeH_4	*C2/c* (196–300)	64	196	[66]
	GeH_3	*Cccm* (280–400)	80	300	[68]
	GeH_8	$P2_1/c$ (220–350)	90	250	[13]
	SnH_4	$P6_3/mmc$ (180–300)	62	200	[71]
	PbH_8	*C2/m* (133–300)	107	230	[73]
Pnictogen	PH_3(exp.)	Uncertain	103	207	[76]
	PH_2	*I4/mmm*	78	220	[77]
	AsH_8	*C2/c* (350–450)	151	450	[80]
	SbH_4	$P6_3/mmc$ (150–300)	118	150	[74]
	BiH_2	$P2_1/m$ (150–300)	65	300	[75]
	BiH_4	*Pmmn* (150–300)	93	150	[75]
	BiH_5	*C2/m* (200–300)	119	300	[75]
	BiH_6	*P-1* (200–300)	113	300	[75]
Chalcogen	H_2S	*Cmca* (160–200)	80	160	[85]
	H_3S	*Im-3m* (180–300)	191–204	200	[17]
	H_3S (exp.)	*Im-3m*	203	155	[19,20]
	H_3Se	*Im-3m* (166–300)	116	200	[92]
	H_5Te_2	*C2/m* (170–300)	58	200	[93]
	H_4Te	$P6_3/mmc$ (162–300)	99	200	[93]
	H_4Po	*C2/c* (137–300)	47	200	[94]
Halogen	H_2Cl	*R-3m* (341–400)	45	450	[101]
	H_2Br	*Cmcm* (240–300)	12	240	[102]
	H_4Br	$P6_3/mmc$ (240–300)	2.4	240	[102]
	H_2I	R-3m (246–300)	33	240	[104]
	H_4I	*P6/mmm* (114–300)	20	150	[105]

ACKNOWLEDGEMENT

The authors would thank the collaborations and discussions with A. R. Oganov, Yanming Ma, Tao Xiao, M. I. Eremets, K. Shimizu and Lanyu Liu.

FUNDING

This work was supported by the National Basic Research Program of China (2011CB808200), National Natural Science Foundation of China (51572108, 11204100, 11574109, 11404134, 11504127), Program for Changjiang Scholars and Innovative Research Team in University (IRT1132), National Found for Fostering Talents of basic Science (J1103202), and Fund for the Doctoral Program of Higher Education (20120061120008).

REFERENCES

1. Onnes HK. The resistance of pure mercury at helium temperatures. *Proc K Ned Akad Wet* 1911; **13**: 1274.
2. Schilling A, Cantoni M and Guo JD *et al.* Superconductivity above 130 K in the Hg-Ba-Ca-Cu-O system. *Nature* 1993; **363**: 56–8.

3. Wu G, Xie YL and Chen H *et al.* Superconductivity at 56 K in samarium-doped SrFeAsF. *J Phys-Condens Matter* 2009; **21**: 142203.
4. Nagamatsu J, Nakagawa N and Muranaka T *et al.* Superconductivity at 39 K in magnesium diboride. *Nature* 2001; **410**: 63–4.
5. Reichlin R, Brister KE and McMahan AK *et al.* Evidence for the insulator-metal transition in xenon from optical, X-ray, and band-structure studies to 170 GPa. *Phys Rev Lett* 1989; **62**: 669–72.
6. Gao L, Xue YY and Chen F *et al.* Superconductivity up to 164 K in $HgBa_2Ca_2Cu_3O_{8+\delta}$ under quasihydrostatic pressures. *Phys Rev B* 1994; **50**: 4260–3.
7. Wigner E and Huntington HB. On the possibility of a metallic modification of hydrogen. *J Chem Phys* 1935; **3**: 764–70.
8. Ashcroft NW. Metallic hydrogen: a high-temperature superconductor? *Phys Rev Lett* 1968; **21**: 1748.
9. Dalladay-Simpson P, Howie RT and Gregoryanz E. Evidence for a new phase of dense hydrogen above 325 gigapascals. *Nature* 2016; **529**: 63–7.
10. Ashcroft NW. Hydrogen dominant metallic alloys: high temperature superconductors? *Phys Rev Lett* 2004; **92**: 187002.
11. Chen XJ, Wang JL and Struzhkin VV *et al.* Superconducting behavior in compressed solid SiH_4 with a layered structure. *Phys Rev Lett* 2008; **101**: 077002.
12. Li YW, Gao GY and Xie Y *et al.* Superconductivity at ∼100 K in dense $SiH_4(H_2)_2$ predicted by first principles. *Proc Natl Acad Sci USA* 2010; **107**: 15708–11.
13. Zhong GH, Zhang C and Chen XJ *et al.* Structural, electronic, dynamical, and superconducting properties in dense $GeH_4(H_2)_2$. *J Phys Chem C* 2012; **116**: 5225–34.
14. Zhou DW, Jin XL and Meng X *et al.* Ab initio study revealing a layered structure in hydrogen-rich KH_6 under high pressure. *Phys Rev B* 2012; **86**: 014118.
15. Wang H, John ST and Tanaka K *et al.* Superconductive sodalite-like clathrate calcium hydride at high pressures. *Proc Natl Acad Sci USA* 2012; **109**: 6463–6.
16. Eremets MI, Trojan IA and Medvedev SA *et al.* Superconductivity in hydrogen dominant materials silane. *Science* 2008; **319**: 1506–9.
17. Duan DF, Liu YX and Tian FB *et al.* Pressure-induced metallization of dense $(H_2S)_2H_2$ with high-T_c superconductivity. *Sci Rep* 2014; **4**: 6968.
18. Duan DF, Huang XL and Tian FB *et al.* Pressure-induced decomposition of solid hydrogen sulfide. *Phys Rev B* 2015; **91**: 180502.
19. Drozdov AP, Eremets MI and Troyan IA *et al.* Conventional superconductivity at 203 kelvin at high pressures in the sulfur hydride system. *Nature* 2015; **525**: 73–6.
20. Einaga M, Sakata M and Ishikawa T *et al.* Crystal structure of the superconducting phase of sulfur hydride. *Nat Phys* 2016; **12**: 835–8.
21. Mazin II. Superconductivity: extraordinarily conventional. *Nature* 2015; **525**: 40–1.
22. Xie Y, Li Q and Oganov AR *et al.* Superconductivity of lithium-doped hydrogen under high pressure. *Acta Crystallogr C Struct Chem* 2014; **70**: 104–11.
23. Pepin C, Loubeyre P and Occelli F *et al.* Synthesis of lithium polyhydrides above 130 GPa at 300 K. *Proc Natl Acad Sci USA* 2015; **112**: 7673–6.
24. Struzhkin VV, Kim D and Stavrou E *et al.* Synthesis of sodium polyhydrides at high pressures. *Nat Comm* 2016; **7**: 12267.
25. Zurek E, Hoffmann R and Ashcroft NW *et al.* A little bit of lithium does a lot for hydrogen. *Proc Natl Acad Sci USA* 2009; **106**: 17640–3.
26. Howie RT, Narygina O and Guillaume CL *et al.* High-pressure synthesis of lithium hydride. *Phys Rev B* 2012; **86**: 064108.
27. Baettig P and Zurek E. Pressure-stabilized sodium polyhydrides: NaH_n ($n > 1$). *Phys Rev Lett* 2011; **106**: 237002.
28. Hooper J and Zurek E. High pressure potassium polyhydrides: a chemical perspective. *J Phys Chem C* 2012; **116**: 13322–8.
29. Hooper J and Zurek E. Rubidium polyhydrides under pressure: emergence of the linear H_3^- species. *Chem Eur J* 2012; **18**: 5013–21.
30. Shamp A, Hooper J and Zurek E. Compressed cesium polyhydrides: Cs^+ sublattices and H_3^- three-connected nets. *Inorg Chem* 2012; **51**: 9333–42.
31. Hooper J, Altintas B and Shamp A *et al.* Polyhydrides of the alkaline earth metals: a look at the extremes under pressure. *J Phys Chem C* 2013; **117**: 2982–92.
32. Yu SY, Zeng QF and Oganov AR *et al.* Exploration of stable compounds, crystal structures, and superconductivity in the Be-H system. *AIP Adv* 2014; **4**: 107118.
33. Wang ZW, Yao YS and Zhu L *et al.* Metallization and superconductivity of BeH_2 under high pressure. *J Chem Phys* 2014; **140**: 124707.
34. Lonie DC, Hooper J and Altintas B *et al.* Metallization of magnesium polyhydrides under pressure. *Phys Rev B* 2013; **87**: 054107.
35. Hooper J, Terpstra T and Shamp A *et al.* Composition and constitution of compressed strontium polyhydrides. *J Phys Chem C* 2014; **118**: 6433–47.
36. Wang YC, Wang H and Tse JS *et al.* Structural morphologies of high-pressure polymorphs of strontium hydrides. *Phys Chem Chem Phys* 2015; **17**: 19379–85.
37. Hu CH, Oganov AR and Zhu Q *et al.* Pressure-induced stabilization and insulator-superconductor transition of BH. *Phys Rev Lett* 2013; **110**: 165504.
38. Abe K and Ashcroft NW. Crystalline diborane at high pressures. *Phys Rev B* 2011; **84**: 104118.
39. Gao GY, Wang H and Bergara A *et al.* Metallic and superconducting gallane under high pressure. *Phys Rev B* 2011; **84**: 064118.
40. Liu YX, Duan DF and Tian FB *et al.* Pressure-induced structures and properties in indium hydrides. *Inorg Chem* 2015; **54**: 9924–8.
41. Pickard CJ and Needs RJ. Metallization of aluminum hydride at high pressures: a first-principles study. *Phys Rev B* 2007; **76**: 144114.
42. Goncharenko I, Eremets MI and Hanfland M *et al.* Pressure-induced hydrogen-dominant metallic state in aluminum hydride. *Phys Rev Lett* 2008; **100**: 045504.
43. Rousseau B and Bergara A. Giant anharmonicity suppresses superconductivity in AlH_3 under pressure. *Phys Rev B* 2010; **82**: 104504.
44. Kim DY, Scheicher RH and Ahuja R. Dynamical stability of the cubic metallic phase of AlH_3 at ambient pressure: density functional calculations. *Phys Rev B* 2008; **78**: 100102(R).
45. Hou PG, Zhao XS and Tian FB *et al.* High pressure structures and superconductivity of $AlH_3(H_2)$ predicted by first principles. *Rsc Adv* 2015; **5**: 5096–101.
46. Benedetti LR, Nguyen JH and Caldwell WA *et al.* Dissociation of CH_4 at high pressures and temperatures: diamond formation in giant planet interiors? *Science* 1999; **286**: 100–2.
47. Martinez-Canales M and Bergara A. No evidence of metallic methane at high pressure. *High Press Res* 2006; **26**: 369–75.
48. Feng J, Grochala W and Jaron T *et al.* Structures and potential superconductivity in SiH_4 at high pressure: en route to "metallic hydrogen". *Phys Rev Lett* 2006; **96**: 017006.
49. Pickard CJ and Needs RJ. High-pressure phases of silane. *Phys Rev Lett* 2006; **97**: 045504.
50. Yao YS, Tse JS and Ma YM *et al.* Superconductivity in high-pressure SiH_4. *Europhys Lett* 2007; **78**: 37003.
51. Chen XJ, Struzhkin VV and Song Y *et al.* Pressure-induced metallization of silane. *Proc Natl Acad Sci USA* 2008; **105**: 20–3.
52. Kim DY, Scheicher RH and Lebegue S *et al.* Crystal structure of the pressure-induced metallic phase of SiH_4 from ab initio theory. *Proc Natl Acad Sci USA* 2008; **105**: 16454–9.

53. Martinez-Canales M, Oganov AR and Ma Y *et al.* Novel structures and superconductivity of silane under pressure. *Phys Rev Lett* 2009; **102**: 087005.
54. Cui WW, Shi JM and Liu HY *et al.* Hydrogen segregation and its roles in structural stability and metallization: silane under pressure. *Sci Rep* 2015; **5**: 13039.
55. Zhang HD, Jin XL and Lv YZ *et al.* High-temperature superconductivity in compressed solid silane. *Sci Rep* 2015; **5**: 8845.
56. Degtyareva O, Proctor JE and Guillaume CL *et al.* Formation of transition metal hydrides at high pressures. *Solid State Commun* 2009; **149**: 1583–6.
57. Jin XL, Meng X and He Z *et al.* Superconducting high-pressure phases of disilane. *Proc Natl Acad Sci USA* 2010; **107**: 9969–73.
58. Flores-Livas JA, Amsler M and Lenosky TJ *et al.* High-pressure structures of disilane and their superconducting properties. *Phys Rev Lett* 2012; **108**: 117004.
59. Strobel TA, Somayazulu M and Hemley RJ. Novel pressure-induced interactions in silane-hydrogen. *Phys Rev Lett* 2009; **103**: 065701.
60. Wang SB, Mao HK and Chen XJ *et al.* High pressure chemistry in the H_2-SiH_4 system. *Proc Natl Acad Sci USA* 2009; **106**: 14763–7.
61. Chen XQ, Wang SB and Mao WL *et al.* Pressure-induced behavior of the hydrogen-dominant compound $SiH_4(H_2)_2$ from first-principles calculations. *Phys Rev B* 2010; **82**: 104115.
62. Michel K, Liu YD and Ozolins V. Atomic structure and SiH_4-H_2 interactions of $SiH_4(H_2)_2$ from first principles. *Phys Rev B* 2010; **82**: 174103.
63. Li YW, Gao GY and Li Q *et al.* Orientationally disordered H_2 in the high-pressure van der Waals compound $SiH_4(H_2)_2$. *Phys Rev B* 2010; **82**: 064104.
64. Yao YS and Klug DD. Silane plus molecular hydrogen as a possible pathway to metallic hydrogen. *Proc Natl Acad Sci USA* 2010; **107**: 20893–8.
65. Li Z, Yu W and Jin CQ. First-principles calculation on phase stability and metallization in GeH_4 under pressure. *Solid State Commun* 2007; **143**: 353–7.
66. Gao GY, Oganov AR and Bergara A *et al.* Superconducting high pressure phase of germane. *Phys Rev Lett* 2008; **101**: 107002.
67. Zhang HD, Jin XL and Lv YZ *et al.* Investigation of stable germane structures under high-pressure. *Phys Chem Chem Phys* 2015; **17**: 27630–5.
68. Hou PG, Tian FB and Li D *et al.* Ab initio study of germanium-hydride compounds under high pressure. *Rsc Adv* 2015; **5**: 19432–8.
69. Strobel TA, Chen XJ and Somayazulu M *et al.* Vibrational dynamics, intermolecular interactions, and compound formation in GeH_4–H_2 under pressure. *J Chem Phys* 2010; **133**: 164512.
70. Tse JS, Yao YS and Tanaka K. Novel superconductivity in metallic SnH_4 under high pressure. *Phys Rev Lett* 2007; **98**: 117004.
71. Gao GY, Oganov AR and Li PF *et al.* High-pressure crystal structures and superconductivity of Stannane (SnH_4). *Proc Natl Acad Sci USA* 2010; **107**: 1317–20.
72. Zaleski-Ejgierd P, Hoffmann R and Ashcroft NW. High pressure stabilization and emergent forms of PbH_4. *Phys Rev Lett* 2011; **107**: 037002.
73. Cheng Y, Zhang C and Wang TT *et al.* Pressure-induced superconductivity in H_2-containing hydride $PbH_4(H_2)_2$. *Sci Rep* 2015; **5**: 16475.
74. Ma YB, Duan DF and Li D *et al.* The unexpected binding and superconductivity in SbH_4 at high pressure. 2015; arXiv:1506.03889.
75. Ma YB, Duan DF and Li D *et al.* High-pressure structures and superconductivity of bismuth hydrides. 2015; arXiv:1511.05291.
76. Drozdov AP, Eremets MI and Troyan IA. Superconductivity above 100 K in PH_3 at high pressures. 2015; arXiv:1508.06224.
77. Shamp A, Terpstra T and Bi T *et al.* Decomposition products of phosphine under pressure: PH_2 stable and superconducting? *J Am Chem Soc* 2016; **138**: 1884–92.
78. Liu HY, Li YW and Gao GY *et al.* Crystal structure and superconductivity of PH_3 at high pressures. *J Phys Chem C* 2016; **120**: 3458–61.
79. Flores-Livas JA, Amsler M and Heil C *et al.* Superconductivity in metastable phases of phosphorus-hydride compounds under high pressure. *Phys Rev B* 2016; **93**: 020508.
80. Fu YH, Du XP and Zhang LJ *et al.* High-pressure phase stability and superconductivity of pnictogen hydrides and chemical trends for compressed hydrides. *Chem Mater* 2016; **28**: 1746–55.
81. Salzmann CG, Radaelli PG and Mayer E *et al.* Ice XV: a new thermodynamically stable phase of ice. *Phys Rev Lett* 2009; **103**: 105701.
82. Wang YC, Liu HY and Lv J *et al.* High pressure partially ionic phase of water ice. *Nat Commun* 2011; **2**: 563.
83. Sakashita M, Yamawaki H and Fujihisa H *et al.* Pressure-induced molecular dissociation and metallization in hydrogen-bonded H_2S solid. *Phys Rev Lett* 1997; **79**: 1082–5.
84. Wang LC, Tian FB and Feng WX *et al.* Order-disorder phase transition and dissociation of hydrogen sulfide under high pressure: ab initio molecular dynamics study. *J Chem Phys* 2010; **132**: 164506.
85. Li YW, Hao J and Liu HY *et al.* The metallization and superconductivity of dense hydrogen sulfide. *J Chem Phys* 2014; **140**: 174712.
86. Strobel TA, Ganesh P and Somayazulu M *et al.* Novel cooperative interactions and structural ordering in H_2S-H_2. *Phys Rev Lett* 2011; **107**: 255503.
87. Bernstein N, Hellberg CS and Johannes MD *et al.* What superconducts in sulfur hydrides under pressure and why. *Phys Rev B* 2015; **91**: 060511.
88. Errea I, Calandra M and Pickard CJ *et al.* High-pressure hydrogen sulfide from first principles: a strongly anharmonic phonon-mediated superconductor. *Phys Rev Lett* 2015; **114**: 157004.
89. Quan Y and Pickett WE. Van Hove singularities and spectral smearing in high-temperature superconducting H_3S. *Phys Rev B* 2016; **93**: 104526.
90. Heil C and Boeri L. Influence of bonding on superconductivity in high-pressure hydrides. *Phys Rev B* 2015; **92**: 060508.
91. Ge YF, Zhang F and Yao YG. First-principles demonstration of superconductivity at 280 K in hydrogen sulfide with low phosphorus substitution. *Phys Rev B* 2016; **93**: 224513.
92. Zhang ST, Wang YC and Zhang JR *et al.* Phase diagram and high-temperature superconductivity of compressed selenium hydrides. *Sci Rep* 2015; **5**: 15433.
93. Zhong X, Wang H and Zhang JR *et al.* Tellurium hydrides at high pressures: high-temperature superconductors. *Phys Rev Lett* 2016; **116**: 057002.
94. Liu YX, Duan DF and Tian FB *et al.* Prediction of stoichiometric PoH_n compounds: crystal structures and properties. *Rsc Adv* 2015; **5**: 103445–50.
95. Zhang LJ, Wang YC and Zhang XX *et al.* High-pressure phase transitions of solid HF, HCl, and HBr: an ab initio evolutionary study. *Phys Rev B* 2010; **82**: 014108.
96. Chen CB, Xu Y and Sun XP *et al.* Novel superconducting phases of HCl and HBr under high pressure: an ab initio study. *J Phys Chem C* 2015; **119**: 17039–43.
97. Duan DF, Tian FB and He Z *et al.* Hydrogen bond symmetrization and superconducting phase of HBr and HCl under high pressure: an ab initio study. *J Chem Phys* 2010; **133**: 074509.
98. Ikram A, Torrie BH and Powell BM. Structures of solid deuterium bromide and deuterium iodide. *Mol Phys* 1993; **79**: 1037–49.
99. Duan DF, Huang XL and Tian FB *et al.* Predicted formation of H_3^+ in solid halogen polyhydrides at high pressures. *J Phys Chem A* 2015; **119**: 11059–65.
100. Wang ZW, Wang H and Tse JS *et al.* Stabilization of H_3^+ in the high pressure crystalline structure of H_nCl ($n = 2$–7). *Chem Sci* 2015; **6**: 522–6.

101. Zeng QF, Yu SY and Li D *et al.* Emergence of novel hydrogen chlorides under high pressure. 2015; arXiv:1508.01395.
102. Duan DF, Tian FB and Huang XL *et al.* Decomposition of solid hydrogen bromide at high pressure. 2015; arXiv:1504.01196.
103. Katoh E, Yamawaki H and Fujihisa H *et al.* Raman and infrared study of phase transitions in solid HBr under pressure. *Phys Rev B* 1999; **59**: 11244.
104. Duan DF, Tian FB and Liu YX *et al.* Enhancement of T_c in the atomic phase of iodine-doped hydrogen at high pressures. *Phys Chem Chem Phys* 2015; **17**: 32335–40.
105. Shamp A and Zurek E. Superconducting high-pressure phases composed of hydrogen and iodine. *J Phys Chem Lett* 2015; **6**: 4067–72.